Check for updates

View Article Online
View Journal

Journal of
Materials Chemistry A

Accepted Manuscript

This article can be cited before page numbers have been issued, to do this please use: G. Hu, Z. Wu and D. Jiang, *J. Mater. Chem. A*, 2018, DOI: 10.1039/C8TA00461G.

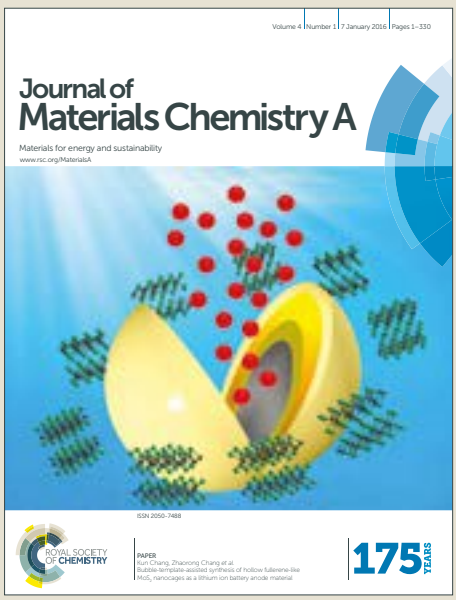

This is an Accepted Manuscript, which has been through the Royal Society of Chemistry peer review process and has been accepted for publication.

Accepted Manuscripts are published online shortly after acceptance, before technical editing, formatting and proof reading. Using this free service, authors can make their results available to the community, in citable form, before we publish the edited article. We will replace this Accepted Manuscript with the edited and formatted Advance Article as soon as it is available.

You can find more information about Accepted Manuscripts in the author guidelines.

Please note that technical editing may introduce minor changes to the text and/or graphics, which may alter content. The journal's standard Terms & Conditions and the ethical guidelines, outlined in our author and reviewer resource centre, still apply. In no event shall the Royal Society of Chemistry be held responsible for any errors or omissions in this Accepted Manuscript or any consequences arising from the use of any information it contains.

ROYAL SOCIETY OF CHEMISTRY

rsc.li/materials-a

Journal of Materials Chemistry A
View Article Online
DOI: 10.1039/C8TA00461G

Published on 19 March 2018. Downloaded by OAKRIDGE NATIONAL LABORATORY on 04/04/2018 16:20:42.

Stronger-than-Pt hydrogen adsorption in a Au_{22} nanocluster for hydrogen evolution reaction

Guoxiang Hu,[†] Zili Wu,[‡] and De-en Jiang*,[†]

[†]Department of Chemistry, University of California, Riverside, California 92521, US

[‡]Chemical Sciences Division and Center for Nanophase Materials Sciences, Oak Ridge National Laboratory, Oak Ridge, Tennessee 37831, US

*To whom correspondence should be addressed. E-mail: djiang@ucr.edu.

Abstract: Atomically-precise metal nanocluster have recently emerged as a novel class of catalysts for hydrogen evolution reaction. From first-principles density functional theory, we show that the eight coordinatively unsaturated (*cus*) Au atoms in the $Au_{22}(L^8)_6$ cluster [L = 1,8-bis(diphenylphosphino) octane] can adsorb H stronger than Pt, thereby being a potentially promising catalyst for hydrogen evolution reaction (HER). We find that up to six H atoms can adsorb on the $Au_{22}(L^8)_6$ cluster and they all have close-to-zero Gibbs free adsorption energies (ΔG_H). From the HOMO-LUMO gaps, frontier orbitals, and Bader charge analysis, we conclude that H behaves as a hydride or electron-withdrawing ligand in the $Au_{22}(L^8)_6$ clusters, in contrast with the metallic H in thiolate-protected Au nanoclusters. Our study demonstrates that ligand-protected Au clusters with *cus* Au sites will be the most promising candidates for realizing Au-H nanoclusters and as excellent electrocatalysts for HER.

Journal of Materials Chemistry A Accepted Manuscript

View Article Online
DOI: 10.1039/C8TA00461G

Published on 19 March 2018. Downloaded by OAKRIDGE NATIONAL LABORATORY on 04/04/2018 16:20:42.

Journal of Materials Chemistry A Accepted Manuscript

Introduction

The behavior of H in metals has been of great interest for many decades.[1-3] Metal-hydrogen systems are widely utilized in energy-storage systems, sensor applications, as well as catalysis.[4] In contrast with bulk metal hydrides, the structures of H-metal nanoclusters can provide insight from a molecular perspective of how H interacts with metals and how the magic sizes or superatoms evolve.[5] The hydride ligand has been used in the synthesis of ligand-protected Cu or Ag nanoclusters.[6-13] Especially for the Cu clusters, a series of air- and moisture-stable Cu hydride clusters ranging from Cu_7H to $Cu_{32}H_{20}$ have been successfully synthesized and the structures have been determined.[14] More recently, three new hydride-rich Ag clusters, $[Ag_{18}H_{16}(TPP)_{10}]^{2+}$, $[Ag_{25}H_{22}(DPPE)_8]^{3+}$, and $[Ag_{26}H_{22}(TFPP)_{13}]^{2+}$, have been synthesized.[15]

Atomically precise Au nanoclusters have attracted intensive research interest over the past two decades due to their potential applications in catalysis, biology, and nanotechnology.[16-18] However, to the best of our knowledge, H has not been observed in ligand-protected Au nanoclusters, but some intermediate states of H adsorbed in thiolate-protected Au clusters have been proposed to explain their roles in the hydrogen evolution reaction (HER).[19] It has been shown that both $Au_{25}(SR)_{18}$ and $PtAu_{24}(SR)_{18}$ exhibit high HER activity and the activity of $PtAu_{24}(SR)_{18}$ is much higher than that of $Au_{25}(SR)_{18}$. In fact, $PtAu_{24}(SR)_{18}$ is among the most active molecular catalysts for HER. To understand the underlying reason, the behavior of H in $[Au_{25}(SR)_{18}]^q$ and mono-atom-doped bimetallic $[M_1Au_{24}(SR)_{18}]^q$ clusters including $PtAu_{24}(SR)_{18}$ has been investigated.[20] It was found that H behaves as a metal in these clusters and contributes its 1s electron to the superatomic free-electron count. But H adsorption is still uphill for at least 200 meV in free energy on these Au clusters, indicating their thermodynamic

View Article Online
DOI: 10.1039/C8TA00461G

Published on 19 March 2018. Downloaded by OAKRIDGE NATIONAL LABORATORY on 04/04/2018 16:20:42.

instability. One strategy to drive down the free energy is to create the coordinatively unsaturated (*cus*) or *in situ* uncoordinated sites in the Au clusters.

Unlike many other clusters where the surface Au atoms are fully coordinated by the protecting ligands,[21-24] the $Au_{22}(L^8)_6$ cluster (L = 1,8-bis(diphenylphosphino) octane) is unique in that it contains eight *cus* or so-called in situ uncoordinated Au atoms.[25] As shown in Fig. 1, the rod-like Au_{22} core of the $Au_{22}(L^8)_6$ cluster consists of two Au_{11} units clipped together by four L^8 ligands (ball-and-stick ligands in Fig. 1a), while the additional two ligands each coordinate to a Au_{11} unit in a bidentate fashion. Significantly, eight Au atoms (highlighted in red in Fig. 1b) at the interface of the two Au_{11} units are not coordinated by any ligands. The presence of the *cus* Au atoms is promising for catalysis. For example, it was found that the intact $Au_{22}(L^8)_6$ nanoclusters readily catalyze CO oxidation at room temperature; DFT modeling of adsorption of CO and O_2 suggested that the *cus* Au atoms are the active sites.[26]

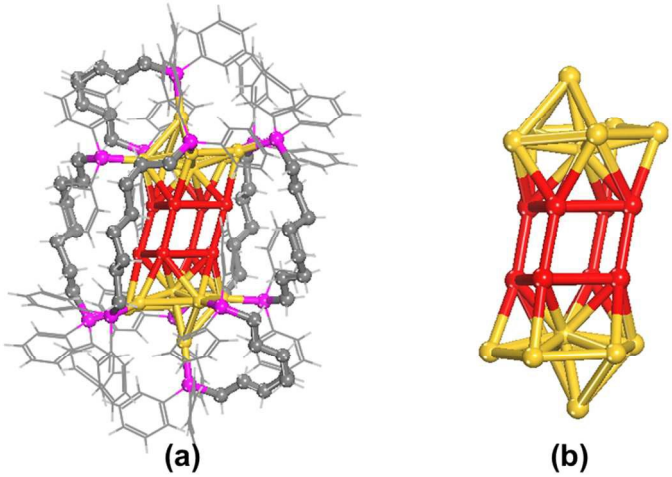

Fig. 1 Total structure (a) and core structure (b) of the $Au_{22}(L^8)_6$ cluster. *Cus* Au, red; other Au, yellow; P, magenta; C, grey; H, light grey.

Due to its many *cus* Au sites, we hypothesize that $Au_{22}(L^8)_6$ offers a unique opportunity to observe H in Au nanoclusters and can be an excellent electrocatalyst for HER. To test this hypothesis, here we studied the structures and energetics of H adsorption on the $Au_{22}(L^8)_6$ cluster

Journal of Materials Chemistry A Accepted Manuscript

View Article Online
DOI: 10.1039/C8TA00461G

Published on 19 March 2018. Downloaded by OAKRIDGE NATIONAL LABORATORY on 04/04/2018 16:20:42.

by first-principles density functional theory (DFT) and evaluated the Gibbs free energies of H adsorption (ΔG_H) to predict the HER activity. In addition, the HOMO-LUMO gaps, frontier orbitals, and partial atomic charges of the H-adsorbed $Au_{22}(L^8)_6$ clusters were analyzed to better understand the behavior of H in the cluster.

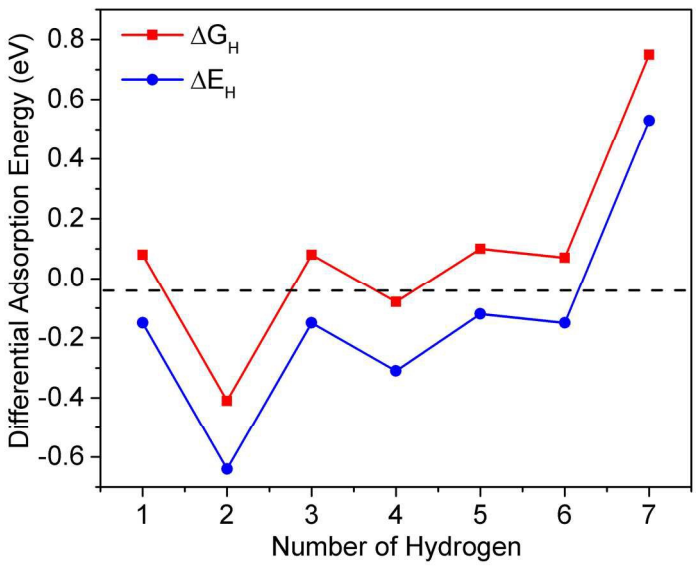

Fig. 2 Differential adsorption energy ΔE_H (blue) and adsorption free energy ΔG_H (red) as a function of number of hydrogen adsorbed on the $Au_{22}(L^8)_6$ cluster.

Results and discussion

Energetics and structures of H adsorption on the $Au_{22}(L^8)_6$ cluster. To find the optimal adsorption sites of H, we tested all the possible sites on the Au_{22} cluster, including top, vertical-bridge, horizontal-bridge, and hollow sites on the Au_8 cube at the center of the cluster (highlighted in red in Fig. 1) as well as the top, bridge, and hollow sites on the two Au_{11} units (highlighted in yellow in Fig. 1). The H atoms first adsorb at the lowest energy sites, and then fill the next lowest and so on.

Fig. 2 shows the calculated differential H adsorption energy (ΔE_H; blue) and free energy (ΔG_H; red) on the $Au_{22}(L^8)_6$ cluster relative to ½ H_2. One can see that up to six H atoms can be

Journal of Materials Chemistry A Accepted Manuscript

View Article Online
DOI: 10.1039/C8TA00461G

Published on 19 March 2018. Downloaded by OAKRIDGE NATIONAL LABORATORY on 04/04/2018 16:20:42.

Journal of Materials Chemistry A Accepted Manuscript

favorably adsorbed on the cluster, while the second H binds strongest. ΔG_H has been considered as a good descriptor for HER and a close-to-zero ΔG_H would suggest a good HER catalyst.[27] One can see that ΔG_H on the $Au_{22}(L^8)_6$ cluster is close-to-zero for the first six H atoms, except the second one. This result has two important implications: (i) the two-H state or $Au_{22}H_2(L^8)_6$ cluster is highly favorable and probably can be detected experimentally; (ii) the $Au_{22}(L^8)_6$ cluster should be a highly active HER catalyst since it offers so many sites that have close-to-zero ΔG_H. For comparison, we have also calculated ΔG_H on the Pt(111) surface (at the same level of theory and with the same approach) and found it to be -0.14 eV. Hence, the second H adsorption on the $Au_{22}(L^8)_6$ cluster (ΔG_H = -0.41 eV) is much stronger than H adsorption on the Pt(111) surface, indicating the high stability of the $Au_{22}H_2(L^8)_6$ cluster.

H adsorption on the $Au_{22}(L^8)_6$ cluster shown in Fig. 2 is drastically different from previously studied $[Au_{25}(SR)_{18}]^q$ and mono-atom-doped bimetallic $[M_1Au_{24}(SR)_{18}]^q$ clusters.[20] For the thiolate-protected Au clusters, all the surface gold atoms are protected by thiolate ligands already, so there is no *cus* Au site. As a result, the bonding of H in thiolate-protected Au clusters is generally weaker (ΔG_H > 0.200 eV) than in the $Au_{22}(L^8)_6$ cluster (ΔG_H ~ -0.40 to 0.10 eV).

To understand the energetic pattern of H adsorption on the $Au_{22}(L^8)_6$ cluster, we now examine the optimized structures. One can see from Fig. 3 that the first H atom adsorbs at the vertical-bridge site formed by two *cus* Au atoms, while the second H atom also adsorbs at the vertical-bridge site on the opposite side of the Au_8 cube. Then the third and the fourth H atoms occupy the other two vertical-bridge sites subsequently. Interestingly, the fifth and the six H atoms adsorb at the bridge sites at the opposite ends of the cluster where the Au atoms are not *cus* sites but protected by phosphine ligands. If the first H atom directly adsorbs at the non-*cus*-Au bridge site, ΔG_H is 0.87 eV. In other words, H adsorption at the *cus* Au sites can activate the

View Article Online
DOI: 10.1039/C8TA00461G

Published on 19 March 2018. Downloaded by OAKRIDGE NATIONAL LABORATORY on 04/04/2018 16:20:42.

non-*cus* Au sites; the interaction between H atoms and non-*cus* Au atoms becomes stronger after four H adsorb at the *cus* Au sites. What's more intriguing is that each cap with their non-*cus* Au atoms can accommodate only one H atom, because adsorption of the seventh H atom at the non-*cus* Au bridge site is highly unfavorable (Fig. 2). These observations strongly indicate some magic-number nature with compositions of $Au_{22}H_2(L^8)_6$ and $Au_{22}H_6(L^8)_6$ which should correlate with their electronic structure.

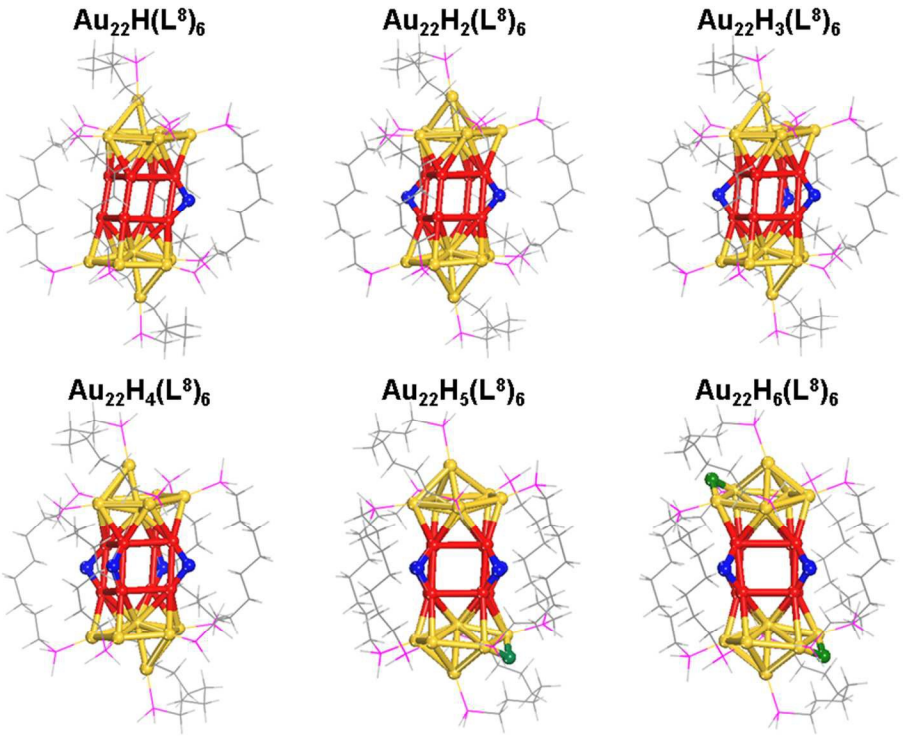

Fig. 3 Optimized structures of the $Au_{22}H_n(L^8)_6$ clusters, n=1~6. Protecting ligands are shown in line mode. *Cus* Au, red; other Au, yellow; H at the *cus* Au sites, blue; H at the non-*cus* Au sites, green; other H, light grey; P, magenta; C, grey.

Journal of Materials Chemistry A Accepted Manuscript

View Article Online
DOI: 10.1039/C8TA00461G

Published on 19 March 2018. Downloaded by OAKRIDGE NATIONAL LABORATORY on 04/04/2018 16:20:42.

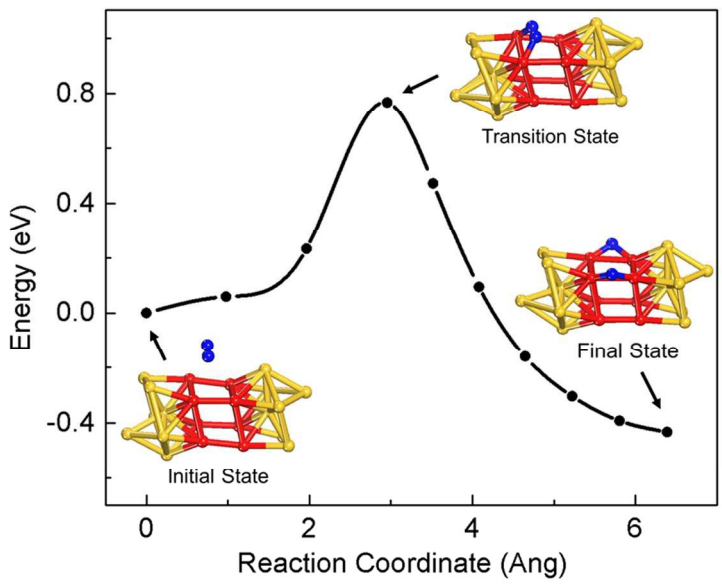

Fig. 4 Minimum-energy path of H_2 dissociation on the $Au_{22}(L^8)_6$ cluster. Structures for initial, transition, and final states are also shown. The protecting ligands are eliminated for clarity. *Cus* Au, red; other Au, yellow; H, blue.

Another interesting implication from the highly stable $Au_{22}H_2(L^8)_6$ cluster is that $Au_{22}(L^8)_6$ can be a good catalyst for H_2 activation. To test this idea, we located the minimum-energy path for H_2 dissociation on the $Au_{22}(L^8)_6$ cluster (Fig. 4) and the barrier was found to be 0.76 eV with a reaction energy of -0.43 eV. One can see that the H_2 molecule dissociates at the short-edge site of the *cus* Au_8 center. After dissociation, H atoms adsorb at two adjacent long-bridge sites. We further calculated the barrier of H diffusion from a long-bridge site to the next to form the configuration as in Fig. 3 for $Au_{22}H_2(L^8)_6$. This barrier was found to be 0.54 eV (ΔE = -0.19 eV). These low barriers indicate that the $Au_{22}(L^8)_6$ cluster should be able to activate H_2 at room temperature.

Partial atomic charges of H in the $Au_{22}(L^8)_6$ clusters. To understand the electronic structure of these clusters, we need to determine their free-electron count. Here a key question is whether H behaves as a hydride or a metal. To solve this issue, we performed Bader charge analysis. We

Journal of Materials Chemistry A Accepted Manuscript

View Article Online
DOI: 10.1039/C8TA00461G

Published on 19 March 2018. Downloaded by OAKRIDGE NATIONAL LABORATORY on 04/04/2018 16:20:42.

found that charges on H in the phosphine-protected $Au_{22}(L^8)_6$ cluster are all negative (ranging from -0.17 to -0.10 |e|), like a hydride. In contract, H in thiolate-protected Au_{25} behaves as a metal with close-to-zero charges.[20] So the behavior of H in Au nanoclusters is ligand-dependent. Due to the electron-donating phosphines, charges on Au are negative (ranging from -0.23 to -0.11 |e|) for the $Au_{22}(L^8)_6$ cluster. Fig. 5 shows the isosurface plot of charge density difference for the $Au_{22}(L^8)_6$ cluster with two adsorbed H. As one can see, electrons accumulate on the adsorbed H, while deplete on the Au atoms bonded to H. Our results of the charge analysis clearly show that H in the phosphine-protected Au nanoclusters behaves as a hydride, different from the metallic H in the thiolate-protected Au nanoclusters.

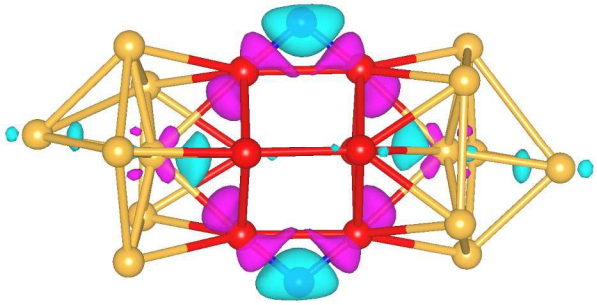

Fig. 5 Charge density difference for the $Au_{22}(L^8)_6$ cluster with two adsorbed H at the contour level of 0.003 eV/Å^3. The charge accumulation region is in light blue and the charge depletion region is in magenta. The protecting ligands are omitted for clarity. *Cus* Au, red; other Au, yellow; H, blue.

HOMO-LUMO gaps and frontier orbitals of the H-adsorbed $Au_{22}(L^8)_6$ clusters. Since H behaves as a hydride, it can localize an electron from the core. By the electron-counting rule from the superatom complex model,[5] the free-electrons of the $Au_{22}H_n(L^8)_6$ clusters (n=0, 2, 4, 6) are shown in Table 1 together with the calculated HOMO-LUMO gaps. Compared with $Au_{22}(L^8)_6$ and $Au_{22}H_2(L^8)_6$, $Au_{22}H_4(L^8)_6$ has a smaller gap. This explained why the second H rather than the fourth H gave the strongest H adsorption (Fig. 2). The $Au_{22}(L^8)_6$ cluster has 22 electrons, which does not correspond to a spherical shell closing. Instead, one can consider that

Journal of Materials Chemistry A Accepted Manuscript

View Article Online
DOI: 10.1039/C8TA00461G

Published on 19 March 2018. Downloaded by OAKRIDGE NATIONAL LABORATORY on 04/04/2018 16:20:42.

Journal of Materials Chemistry A Accepted Manuscript

each of two Au_{11} units contributes three electrons for the bonding between them. The HOMO of $Au_{22}(L^8)_6$ shows significant distribution at the interface between the two Au_{11} units (Fig. 6). $Au_{22}H_2(L^8)_6$ has a more delocalized HOMO, but still with large densities at the interface. However, in the case of $Au_{22}H_4(L^8)_6$, the Au_{11} units do not contribute electrons to the interface. It can be viewed as a "8e +10e" system instead of "9e+9e", because the triplet state is 0.17 eV higher than the singlet state. Accordingly, the HOMO of $Au_{22}H_4(L^8)_6$ is mainly localized on the two Au_{11} units, in the absence of any interactions between them. In addition, the HOMO diagrams also indicate the electron-rich sites that would attract (additional) H atoms.

Table 1 Free-electron counts (N) and HOMO-LUMO gaps of the $Au_{22}H_n(L^8)_6$ clusters, n=0, 2, 4, 6.

Clusters	**$Au_{22}(L^8)_6$**	**$Au_{22}H_2(L^8)_6$**	**$Au_{22}H_4(L^8)_6$**	**$Au_{22}H_6(L^8)_6$**
N	22	20	18	16
Gap /eV	0.716	0.667	0.520	1.185

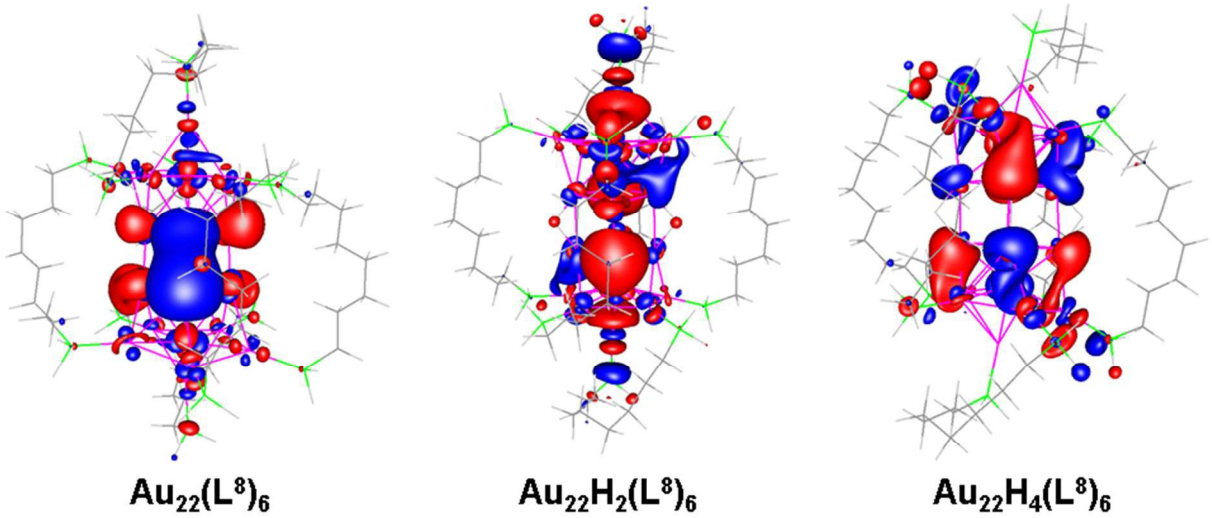

Fig. 6 The HOMO diagrams of $Au_{22}(L^8)_6$, $Au_{22}H_2(L^8)_6$, and $Au_{22}H_4(L^8)_6$ clusters.

View Article Online
DOI: 10.1039/C8TA00461G

Published on 19 March 2018. Downloaded by OAKRIDGE NATIONAL LABORATORY on 04/04/2018 16:20:42.

The $Au_{22}H_6(L^8)_6$ cluster has a much larger gap (1.185 eV). Moreover, the nondegenerate, doubly occupied HOMO of $Au_{22}H_6(L^8)_6$ resembles two spatially separated P-type orbitals, while the LUMO resembles two D-type orbitals (Fig. 7). This suggests that $Au_{22}H_6(L^8)_6$ can be viewed as a "8e+8e" superatom for its 16 free electrons. We also checked the frontier orbitals of another 16-electron system, $[Au_{22}H_4(L^8)_6]^{2+}$. We found that its frontier orbitals have very similar features as $Au_{22}H_6(L^8)_6$ and it also has a very large gap of 1.399 eV. This "8e+8e" superatomic shell-closing is the main reason that the $Au_{22}(L^8)_6$ cluster can absorb up to six H atoms to form the $Au_{22}H_6(L^8)_6$ cluster, even though the last two H atoms have to go to the phosphine-protected gold atoms where the HOMO has more distribution (Fig. 6).

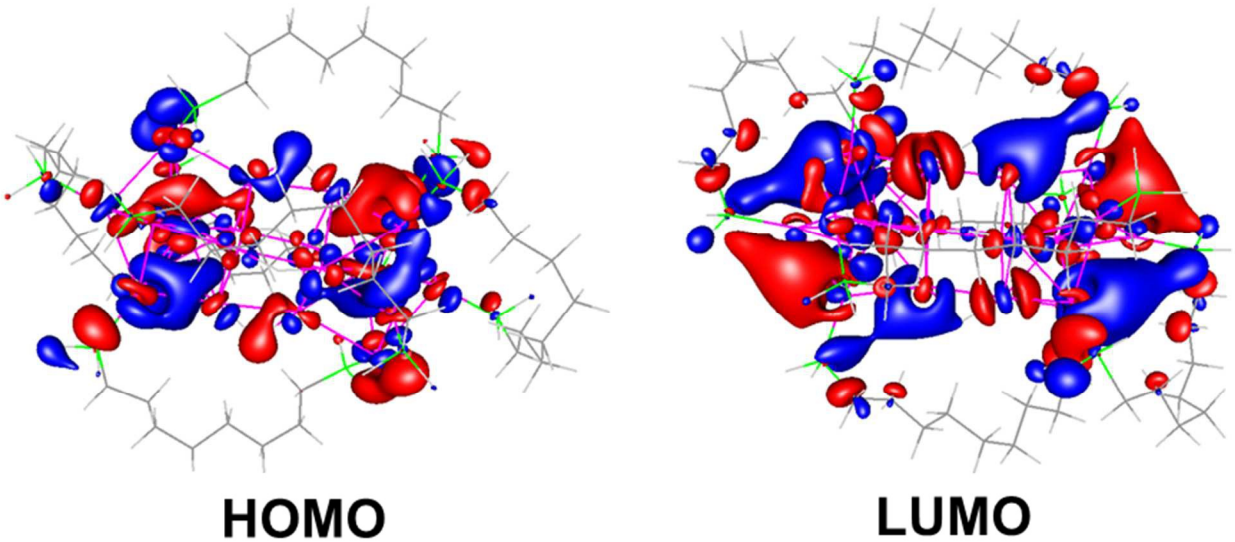

Fig. 7 Frontier orbitals of the $Au_{22}H_6(L^8)_6$ cluster. Only one HOMO and one LUMO are shown.

Journal of Materials Chemistry A Accepted Manuscript

View Article Online
DOI: 10.1039/C8TA00461G

Published on 19 March 2018. Downloaded by OAKRIDGE NATIONAL LABORATORY on 04/04/2018 16:20:42.

It is interesting to investigate the difference in the orbitals below the HOMO, especially in the region of the H atoms, for H-adsorbed $Au_{25}(SR)_{18}$ and $Au_{22}(L^8)_6$ clusters (see Fig. S1 in the electronic supplementary information). The eigenvalue spectra of $Au_{25}H(SR)_{18}$ and $Au_{22}H_2(L^8)_6$ are compared in Fig. S1a,b. One can see that the orbital levels in $Au_{22}H_2(L^8)_6$ have a much lower degeneracy than those in $Au_{25}H(SR)_{18}$, due to the former's lower symmetry. By analyzing the local density of states (Fig. S1c,d), we find that the 1s orbital of H is mainly involved in the HOMO-1 of $Au_{25}H(SR)_{18}$ (Fig. S1e) and HOMO-2 of $Au_{22}H_2(L^8)_6$ (Fig. S1f). One can see that the HOMO-1 of $Au_{25}H(SR)_{18}$ is very delocalized, representing a superatomic P-type orbital, while the HOMO-2 of $Au_{22}H_2(L^8)_6$ is more localized to the *cus* Au atoms in the middle and the two adsorbed H atoms. This orbital picture confirms the difference of hydrogen interaction with $Au_{25}(SR)_{18}$ and $Au_{22}(L^8)_6$: the interaction with $Au_{25}(SR)_{18}$ is dictated by the superatomic electronic structure due to the lack of *cus* Au sites; the interaction with $Au_{22}(L^8)_6$ for the first four H atoms is rather local to and dictated by the eight *cus* Au atoms.

Implications of H adsorption on the $Au_{22}(L^8)_6$ cluster. Our study of H adsorption on the $Au_{22}(L^8)_6$ cluster has important implications. First, our results show that the $Au_{22}H_2(L^8)_6$ cluster is thermodynamically very favorable, suggesting that it may be realized experimentally. This can in principle be realized by just bubbling H_2 gas through a solution of the $Au_{22}H_2(L^8)_6$ cluster. Spectroscopic tools including H-NMR,[28] FT-IR,[29] and inelastic neutron scattering (INS)[30] have been demonstrated the ability in detecting hydride species in both homogeneous gold complexes and heterogeneous gold nanoparticles and can thus be utilized to experimentally verify the ability of $Au_{22}(L^8)_6$ cluster in forming stable hydride species.

Journal of Materials Chemistry A Accepted Manuscript

View Article Online
DOI: 10.1039/C8TA00461G

Published on 19 March 2018. Downloaded by OAKRIDGE NATIONAL LABORATORY on 04/04/2018 16:20:42.

Journal of Materials Chemistry A Accepted Manuscript

Second, the four *cus*-Au and two non-*cus*-Au bridge sites are potentially active sites for HER. The present work focuses on the thermodynamics of H adsorption on the $Au_{22}(L^8)_6$ cluster and its implication for HER. The viability of the cluster for HER will of course depend on the barriers of the Volmer, Heyrovsky, and Tafel steps, which warrant further studies.

Conclusions

In summary, we have investigated how H interacts with the $Au_{22}(L^8)_6$ clusters by DFT calculations. We find that six H can adsorb on the $Au_{22}(L^8)_6$ cluster: four H at the *cus* Au sites, while two H at the non-*cus* sites. More interestingly, most of the adsorbed H possess close-to-zero ΔG_H, indicating that $Au_{22}(L^8)_6$ can be a very good electrocatalyst for HER. In addition, we find that H behaves as a hydride or electron-withdrawing ligand in the $Au_{22}(L^8)_6$ cluster. This is different from the metallic H in thiolate-protected Au nanoclusters, so we conclude that the behavior of H in ligand-protected Au nanoclusters is ligand-dependent. Our study demonstrates the unique behavior of H in atomically precise Au nanoclusters and invite experimental detection of H in these clusters and test of the $Au_{22}(L^8)_6$ cluster for water splitting.

Computational methods

We employed the Vienna *ab initio* simulation package (VASP) to perform DFT calculations with periodic boundary conditions (PBC) and plane-wave bases.[31] We put the cluster in a 30×30×30 $Å^3$ cubic box, and the initial structure of the cluster is form the crystallographic information file provided by the experimental researchers.[25] Phenyl groups were replaced by hydrogens for the purpose of simplifying the calculations. The Perdew−Burke−Ernzerhof (PBE) form of the

View Article Online
DOI: 10.1039/C8TA00461G

Published on 19 March 2018. Downloaded by OAKRIDGE NATIONAL LABORATORY on 04/04/2018 16:20:42.

generalized gradient approximation was used for electron exchange and correlation.[32] The PBE-GGA functional has been demonstrated to achieve a good balance between accuracy and cost for the ligand-protected Au nanoclusters.[33] The ion-electron interaction was described by projector augmented wave (PAW),[34] and the wave function was expanded by plane waves with a cutoff energy of 400 eV. Spin polarization was used for system of odd-number electrons. Geometry relaxations were carried out using the conjugate-gradient algorithm with a criterion that all the residual force components on each atom are less than 0.03 eV/ Å. Γ point only was used to sample the k space. Partial atomic charges were obtained using Bader charge analysis as implemented by Henkelman and co-workers.[35] The climbing-image nudged elastic band (CI-NEB) method implemented in VASP was used to determine the energy barriers.[36] The transition states were obtained by relaxing the force below 0.05 eV/Å. Periodic DFT calculations at the same level of theory were performed for the Pt(111) surface.

The Pt(111) surface was modeled with four layers of slab in (4 × 4) lateral cells, and with 15 Å of vacuum along the z-direction. During the structure optimizations, the top two layers of the slab were allowed to relax together with the adsorbed H.

The frontier orbitals were generated from the Turbomole program (Version 6.5)[37] without the periodic boundary conditions at the same DFT-PBE level with the def2-SVP basis sets,[38] and a scalar-relativistic effective-core potential with 60 core electrons was used for Au.[39]

The differential hydrogen adsorption energy ΔE_H was calculated by

$$\Delta E_H = E(catalyst + nH) - E[catalyst + (n-1)H] - \frac{1}{2}E(H_2) \quad (1)$$

where $E(catalyst + nH)$ and $E[catalyst + (n-1)H]$ represent the total energies of the catalyst with n and n-1 adsorbed H, respectively. $E(H_2)$ represents the total energy of a gas

Journal of Materials Chemistry A Accepted Manuscript

View Article Online
DOI: 10.1039/C8TA00461G

Published on 19 March 2018. Downloaded by OAKRIDGE NATIONAL LABORATORY on 04/04/2018 16:20:42.

phase H_2 molecule. A negative value of ΔE_H suggests favorable absorption. The differential Gibbs free energy of hydrogen adsorption ΔG_H was obtained by

$$\Delta G_H = \Delta E_H + \Delta E_{ZPE} - T\Delta S_H \quad (2)$$

where ΔE_{ZPE} is the difference in zero-point energy between the adsorbed H and H in the gas phase H_2 molecule, and ΔS_H is the entropy difference between the adsorbed H and $\frac{1}{2}H_2$ in the gas phase at the standard condition. The zero-point energy was calculated by summing vibrational frequencies ω_ν over all normal modes ν: $E_{ZPE} = \frac{1}{2}\sum \hbar\omega_\nu$. The entropy of the free H_2 molecule at 298.15 K and 1 atm was taken from the NIST database,[40] while for the adsorbed H, the vibrational entropy was considered and calculated by the methods described by Cramer.[41]

Acknowledgements

This work was supported by the U.S. Department of Energy (DOE), Office of Science, Office of Basic Energy Sciences, Chemical Sciences, Geosciences, and Biosciences Division. This research used resources of the National Energy Research Scientific Computing Center, a DOE Office of Science User Facility supported by the Office of Science of the U.S. Department of Energy under Contract DE-AC02-05CH11231.

Electronic supplementary information (ESI) available: Comparison of $Au_{25}H(SR)_{18}$ and $Au_{22}H_2(L^8)_6$ clusters in terms of eigenvalue spectra; the local density of states; H-involving orbitals.

References

1 R. Mohtadi and S. Orimo, *Nat. Rev. Mater.*, 2016, **2**, 16091.
2 A. J. Jordan, G. Lalic and J. P. Sadighi, *Chem. Rev.*, 2016, **116**, 8318-8372.

Journal of Materials Chemistry A Accepted Manuscript

View Article Online
DOI: 10.1039/C8TA00461G

Published on 19 March 2018. Downloaded by OAKRIDGE NATIONAL LABORATORY on 04/04/2018 16:20:42.

3 R. N. Perutz and B. Procacci, *Chem. Rev.*, 2016, **116**, 8506-8544.

4 A. Pundt and R. Kirchheim, *Annu. Rev. Mater. Res.*, 2006, **36**, 555-608.

5 M. Walter, J. Akola, O. Lopez-Acevedo, P. D. Jadzinsky, G. Calero, C. J. Ackerson, R. L. Whetten, H. Grönbeck and H. Häkkinen, *Proc. Natl. Acad. Sci.*, 2008, **105**, 9157-9162.

6 S. A. Bezman, M. R. Churchill, J. A. Osborn and J. Wormald, *J. Am. Chem. Soc.*, 1971, **93**, 2063-2065.

7 T. H. Lemmen, K. Folting, J. C. Huffman and K. G. Caulton, *J. Am. Chem. Soc.*, 1985, **107**, 7774-7775.

8 C. Liu, B. Sarkar, Y. J. Huang, P. K. Liao, J. C. Wang, J. Y. Saillard and S. Kahlal, *J. Am. Chem. Soc.*, 2009, **131**, 11222-11233.

9 R. S. Dhayal, J. H. Liao, Y. R. Lin, P. K. Liao, S. Kahlal, J. Y. Saillard and C. Liu, *J. Am. Chem. Soc.*, 2013, **135**, 4704-4707.

10 A. Zavras, G. N. Khairallah, T. U. Connell, J. M. White, A. J. Edwards, P. S. Donnelly and R. A. O'Hair, *Angew. Chem. Int. Ed.*, 2013, **52**, 8391-8394.

11 A. J. Edwards, R. S. Dhayal, P. K. Liao, J. H. Liao, M. H. Chiang, R. O. Piltz, S. Kahlal, J. Y. Saillard and C. Liu, *Angew. Chem. Int. Ed.*, 2014, **53**, 7214-7218.

12 T. D. Nguyen, Z. R. Jones, B. R. Goldsmith, W. R. Buratto, G. Wu, S. L. Scott and T. W. Hayton, *J. Am. Chem. Soc.*, 2015, **137**, 13319-13324.

13 S. Daly, M. Krstić, A. Giuliani, R. Antoine, L. Nahon, A. Zavras, G. N. Khairallah, V. Bonačić-Koutecký, P. Dugourd and A. Richard, *Phys. Chem. Chem. Phys.*, 2015, **17**, 25772-25777.

14 R. S. Dhayal, W. E. van Zyl and C. Liu, *Acc. Chem. Res.*, 2015, **49**, 86-95.

15 M. S. Bootharaju, R. Dey, L. E. Gevers, M. N. Hedhili, J. M. Basset and O. M. Bakr, *J. Am. Chem. Soc.*, 2016, **138**, 13770-13773.

16 R. Jin, C. Zeng, M. Zhou and Y. Chen, *Chem. Rev.*, 2016, **116**, 10346-10413.

17 J. Fang, B. Zhang, Q. Yao, Y. Yang, J. Xie and N. Yan, *Coord. Chem. Rev.* , 2016, **322**, 1-29.

18 I. Chakraborty and T. Pradeep, *Chem. Rev.* , 2017, **117**, 8208-8271.

19 K. Kwak, W. Choi, Q. Tang, M. Kim, Y. Lee, D. E. Jiang and D. Lee, *Nat. Commun.*, 2017, **8**, 14723.

20 G. Hu, Q. Tang, D. Lee, Z. Wu and D. E. Jiang, *Chem. Mater.*, 2017, **29**, 4840-4847.

Journal of Materials Chemistry A Accepted Manuscript

View Article Online
DOI: 10.1039/C8TA00461G

Published on 19 March 2018. Downloaded by OAKRIDGE NATIONAL LABORATORY on 04/04/2018 16:20:42.

Journal of Materials Chemistry A Accepted Manuscript

21 P. D. Jadzinsky, G. Calero, C. J. Ackerson, D. A. Bushnell and R. D. Kornberg, *Science*, 2007, **318**, 430-433.

22 M. W. Heaven, A. Dass, P. S. White, K. M. Holt and R. W. Murray, *J. Am. Chem. Soc.*, 2008, **130**, 3754-3755.

23 M. Zhu, C. M. Aikens, F. J. Hollander, G. C. Schatz and R. Jin, *J. Am. Chem. Soc.*, 2008, **130**, 5883-5885.

24 H. Qian, W. T. Eckenhoff, Y. Zhu, T. Pintauer and R. Jin, *J. Am. Chem. Soc.*, 2010, **132**, 8280-8281.

25 J. Chen, Q. F. Zhang, T. A. Bonaccorso, P. G. Williard and L. S. Wang, *J. Am. Chem. Soc.*, 2013, **136**, 92-95.

26 Z. Wu, G. Hu, D. E. Jiang, D. R. Mullins, Q. F. Zhang, L. F. Allard Jr, L. S. Wang and S. H. Overbury, *Nano Lett.*, 2016, **16**, 6560-6567.

27 J. K. Nørskov, T. Bligaard, A. Logadottir, J. R. Kitchin, J. G. Chen, S. Pandelov and U. Stimming, *J. Electrochem. Soc.*, 2005, **152**, J23-J26.

28 D. A. Roşca, J. Fernandez-Cestau, D. L. Hughes and M. Bochmann, *Organometallics*, 2014, **34**, 2098-2101.

29 R. Juárez, S. F. Parker, P. Concepción, A. Corma and H. García, *Chem. Sci.*, 2010, **1**, 731-738.

30 I. Silverwood, S. Rogers, S. Callear, S. Parker and C. Catlow, *Chem. Commun.*, 2016, **52**, 533-536.

31 G. Kresse and J. Furthmüller, *Phys. Rev. B*, 1996, **54**, 11169-11186.

32 J. P. Perdew, K. Burke and M. Ernzerhof, *Phys. Rev. Lett.* , 1996, **77**, 3865-3868.

33 D. E. Jiang, *Nanoscale*, 2013, **5**, 7149-7160.

34 P. E. Blöchl, *Phys. Rev. B*, 1994, **50**, 17953-17979.

35 W. Tang, E. Sanville and G. Henkelman, *J. Phys. Condens. Matter*, 2009, **21**, 084204.

36 G. Henkelman, B. P. Uberuaga and H. Jónsson, *J. Chem. Phys.*, 2000, **113**, 9901-9904.

37 R. Ahlrichs, M. Bär, M. Häser, H. Horn and C. Kölmel, *Chem. Phys. Lett.*, 1989, **162**, 165-169.

38 A. Schäfer, H. Horn and R. Ahlrichs, *J. Chem. Phys.*, 1992, **97**, 2571-2577.

39 D. Andrae, U. Haeussermann, M. Dolg, H. Stoll and H. Preuss, *Theor. Chim. Acta.*, 1990, **77**, 123-141.

View Article Online
DOI: 10.1039/C8TA00461G

40 NIST Chemistry WebBook, NIST Standard Reference Database Number 69; P. J. Linstrom and W. Mallard, Eds.; National Institute of Standards and Technology: Gaithersburg MD, 2005; 20899.

41 C. J. Cramer, Essentials of Computational Chemistry: Theories and Models, 2nd ed.; Wiley & Sons: Chichester, 2004.

Published on 19 March 2018. Downloaded by OAKRIDGE NATIONAL LABORATORY on 04/04/2018 16:20:42.

Journal of Materials Chemistry A Accepted Manuscript

View Article Online
DOI: 10.1039/C8TA00461G

Published on 19 March 2018. Downloaded by OAKRIDGE NATIONAL LABORATORY on 04/04/2018 16:20:42.

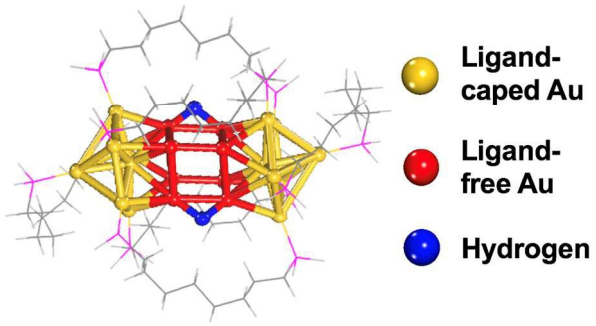

Ligand-protected Au clusters with coordinatively-unsaturated (*cus*) Au atoms are predicted to be promising for realizing Au-H nanoclusters and water splitting.

Journal of Materials Chemistry A Accepted Manuscript